Accuracy Limitations of Perfectly Matched Layers in 3D Finite-Difference Frequency-Domain Method

Thorsten Tischler and Wolfgang Heinrich

Ferdinand-Braun-Institut für Höchstfrequenztechnik (FBH), D-12489 Berlin, Germany

***Abstract* — The perfectly matched layer (PML) boundary condition is employed in conjunction with the 3D finite-difference frequency-domain method (FDFD) for S parameter calculation of microwave devices. We find a residual reflection error, which is related only to discretization at the PML interface. The paper presents a systematic investigation of this parasitic effect and its origin.**

I. Introduction

A variety of absorbing boundary conditions is available for electromagnetic simulation using the finite-difference (FD) or the finite-element (FE) methods. Among these, the Perfectly Matched Layer (PML) proved to be the most powerful formulation so far. Two types of PML are to be distinguished: The split-field formulation, introduced by Berenger [1], and the anisotropic-material based description by Sacks et al. [2]. The anisotropic-material PML formulation offers the special advantage that it can be implemented easily in frequency-domain FD and FE codes and preserves consistency of Maxwellian equations.

The PML formulations and their properties have been the subject of numerous publications (e.g.[3],[4],[5]). Regarding the finite-difference method, however, research focused on the time-domain scheme (FDTD) and only little information is available for the frequency domain (FDFD). Moreover, application of the PML concept in advanced simulation problems requires a detailed knowledge of numerical artifacts and limitations. This is the background for the paper presented here. The objective is to discuss the accuracy limitations when applying the PML in three-dimensional finite-difference frequency-domain (FDFD) simulations. Since the underlying scheme is the same for FDTD and FDFD, the results provide insights into the time-domain behavior as well.

II. Implementation of PML into FDFD

The FDFD method is based on the discrete integral form of the Maxwellian equations applied to each mesh cell

$$\oint_{\partial A} \frac{\vec{B}}{\underline{\mu}} \mathrm{d}\vec{s} = \int_A j\omega \underline{\varepsilon} \vec{E} \mathrm{d}\vec{A}, \quad \oint_{\partial A} \vec{E}\, \mathrm{d}\vec{s} = -\int_A j\omega \vec{B} \mathrm{d}\vec{A}. \qquad (1)$$

The PML formulation chosen is based on the well-known uniaxial permittivity and permeability tensors, [$\underline{\varepsilon}$] and [$\underline{\mu}$], proposed by Sacks et al. [2]. The tensor coefficients $\eta = 1 - j\kappa / (\omega \varepsilon_0)$ introduce a conductivity given by

$$\kappa(z) = \kappa_{\max} \left(\frac{z - z_0}{d} \right)^n, \text{ with } \kappa_{\max} = \frac{(n+1)\varepsilon_0 c_0}{2d} \ln\left[\frac{1}{r_{th}} \right], \qquad (2)$$

for each PM-layer, where n denotes the order of the profile, d represents the thickness of the PML and r_{th} the nominal reflection of the PML region.

III. Code Verification: Calculation of a Dielectric Loaded Waveguide

As a first test of the 3D PML implementation, a waveguide loaded with a dielectric block, according to [5], is calculated (see in Fig. 1).

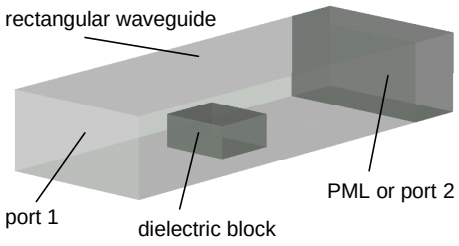

Fig. 1. Perspective view of the structure under consideration: rectangular waveguide (cross section is 20×10mm^2) loaded with a dielectric block (8.88×3.99×8.0 mm^3) with relative permittivity ε_r=6.

Two types of simulations were performed: Using one port (port 1 in Fig. 1) and terminating the waveguide with PML and, to get a reference, substituting the PML by a second port, which leads to an ideal reflection-free termination.

For FDFD calculations a mesh of 11×18×24 cells for the two-port reference and 11×18×29 cells for the PML calculation, respectively, is used. The resulting input reflection S_{11} is plotted in Fig. 2

The agreement between two-port and PML data is excellent. Furthermore, the values correspond to those given in [5]. The PML consists of only five layers, with a chosen nominal reflection coefficient of 0.5% and a constant conductivity profile. Hence, small deviations between the

two-port and the PML results have to be expected. In order to explore this in more detail, we used modifications of the PML, varying the number of layers, the conductivity profile, and the theoretical reflection coefficient.

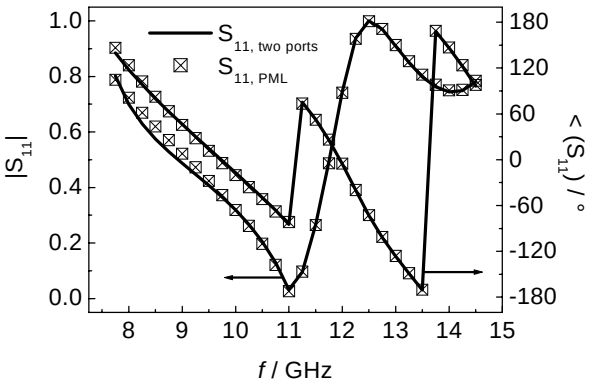

Fig. 2 Input reflection S_{11} of the dielectric-loaded waveguide against frequency; FDFD data using either two ports (lines) or five cells of PML (symbols).

As a point of special interest, the resonance frequency (around 11GHz) was investigated. The results can be summarized as follows: Improving PML properties reduces reflections S_{11}, but a lower limit around –50dB is observed. Interestingly, we obtain a similar level for various other structures, including planar transmission-lines.

In order to have a closer look on this accuracy limitation a simple test structure is treated in the next section.

IV. Test Structure for Reflection Error

In order to avoid all side effects we looked for a test structure, most simple but nevertheless showing the residual reflections we want to study. We find a one-port parallel-plate line (PPL) structure to be most suitable.

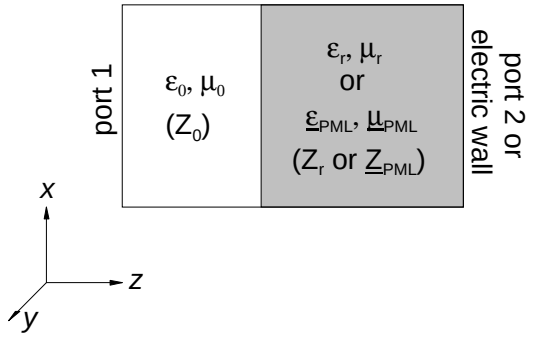

Fig. 3 Test structure for residual reflection errors: parallel-plate waveguide with PML section at the end. The structure is treated either as one-port waveguide, with an electric wall terminating the PML region, or as two-port waveguide.

In the back section, the PPL is filled with PML material, as shown in Fig. 3. The waveguide geometry is x×y×z = 1×1×6mm^3 (1×1×4.8mm^3 for the fully PML filled case, respectively). We apply an equidistant mesh of 12×22×21 cells (12×22×17 cells for the fully PML case). The PML has on overall thickness of 4.8mm, corresponding to 16 cells. The extension of one *z* cell is 0.3mm, corresponding to λ/13 at the highest frequency (75 GHz).

The advantage of this simple structure is that the fields are 1D, which excludes possible *x*,*y*-discretization errors and, furthermore, allows validation by a Mathematica routine. We did not detect, however, remarkable differences between this 1D solution and our 3D FDFD code for any of the simulations.

Fig. 4 presents the results for increasing nominal PML reflection r_{th}.

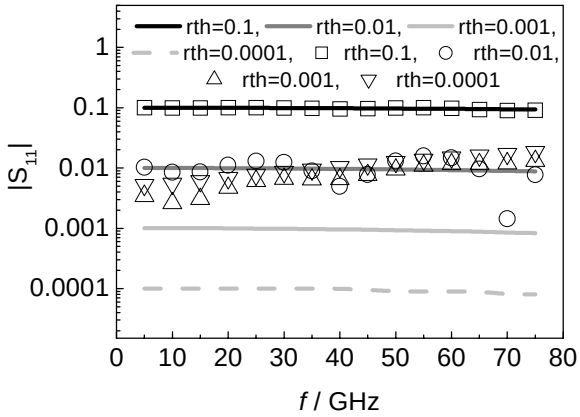

Fig. 4 Input reflection S_{11} of the 1D parallel-plate waveguide of Fig. 3: comparison between results for the waveguide being partly filled with PML (symbols) and results for the waveguide being completely filled with PML material (lines); the parameter r_{th} refers to the PML nominal reflection coefficient.

First, the one-port structure is studied using an electric wall to terminate the PML area. This corresponds to the practical case where the PML is applied to replace an open boundary. As can be seen from Fig. 4 (symbols), reducing the nominal reflection r_{th} leads to lower actual reflection, as long as the resulting S_{11} magnitude is larger than about –50 dB. Further reduction of r_{th} does not improve reflection.

In order to check the PML itself, another calculation is done, filling the waveguide with PML completely (see Fig. 4 (solid curves)). Although all PML parameter are unchanged, now the reflection values reach the chosen nominal r_{th} values, for all frequencies.

In a further investigation, we changed the structure by replacing the electric wall by a second port, thus eliminating any reflections at this boundary. The resulting S_{11} values are plotted in Fig. 5 (lines).

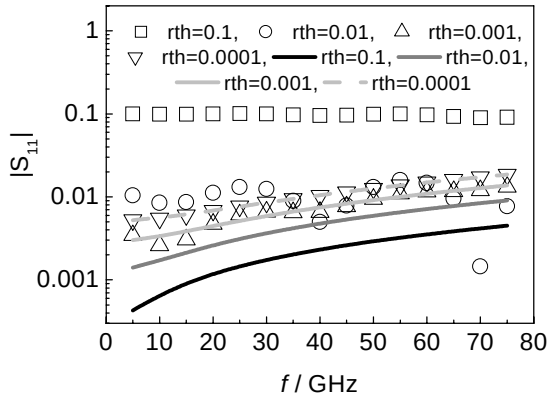

Fig. 5 Input reflection S_{11} of the partly PML-filled waveguide according to Fig. 3; comparison of results using the one-port structure with an electric (symbols) and of the two-port case (lines), where the electric wall is replaced by a second port.

Although one would expect zero reflections, as the PML impedance is inherently equal to that of the air-filled section ($Z_{PML}=Z_0$), there are distinct reflections, which depend on frequency as well as on the reflection coefficient chosen. These residual reflections decrease with growing r_{th}, i.e., with decreasing PML conductivity. Moreover, the two-port calculation of a completely PML filled waveguide results in $S_{11}=0$, for all frequencies and r_{th} values.

From these findings one concludes that the observed reflections are caused neither by the PML nor by numerical dispersion, but only by the transition plane between air and PML. This corresponds to initial observations by Berenger [6] using FDTD in the split-field formulation, but can now be investigated more detailed in the frequency domain.

Regarding Fig. 4, we actually have a point, where the computed reflections overcome the nominal value r_{th}, which is somewhere at $S_{11}\approx0.01$, i.e., –40dB. Given a constant conductivity profile, this level can only be changed by refining the mesh. Therefore, looking for a parameter that allows further reduction of S_{11}, the influence of the conductivity profile is studied in the next section.

V. Influence of Conductivity Profile

As suggested in many papers on PML in FDTD, we applied various conductivity profiles in order to check the influence of this parameter on accuracy limitation. Fig. 6 presents the results for different profiles, ranging from a constant profile (n=0) to an n=5 characteristic. The nominal PML reflection is fixed at $r_{th}=0.0001$. Because of this low value, the data for the different PML terminations (electric wall or second port) do not differ significantly.

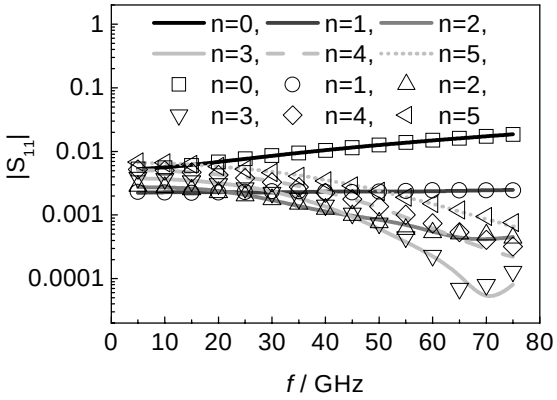

Fig. 6 Input reflection S_{11} of the partly PML-filled waveguide according to Fig. 3; one-port (symbols) and two-port cases (lines), using different conductivity profiles (n=0,1,…,5).

Evaluating the results for different exponents *n* one finds that *n*-values around 3 yield optimum broadband performance, which is in line with previous investigations on FDTD. But, although the grading leads to an improvement of the reflective behavior, it is not possible to reach the desired nominal value r_{th} over the given frequency range. That behavior is different from some published FDTD results (e.g. [4]).

Obviously, the transition air-PML puts a constraint on the minimum values for S_{11}. The question is, whether the parasitic reflections are due to PML-specific characteristics or whether one is dealing with a more general FD phenomenon here. This is clarified in the next section.

VI. Dependence on Discretization

As the last remaining parameter to be investigated, the discretization in *z*-direction is varied. Fig. 7 provides the results.

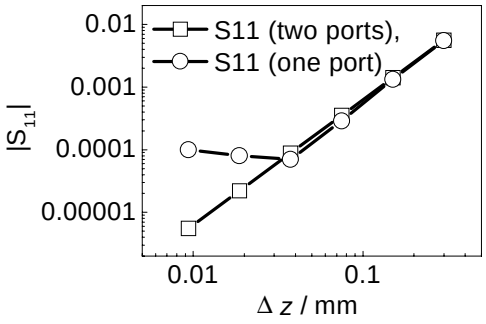

Fig. 7 Input reflection S_{11} of a partly PML filled waveguide according to Fig. 3 as a function of mesh size Δz; results for both one-port and two-port case ($r_{th}=0.0001$, overall length of PML unchanged for all cell sizes, f=10GHz.).

The residual reflection level scales with Δz^2 and converges to the limits as expected, i.e. $S_{11} \rightarrow 0$ for the two-

port, and $S_{11} \rightarrow 0.0001 = r_{th}$ for the one-port case. In other words, increased spatial resolution improves description of the PML interface thus reducing residual reflections.

VII. Analytic Description

The PML material involves two peculiarities of interest here: the presence of both electric and magnetic losses, which is an artificial setting, and a change of both permittivity and permeability at the interface, which can occur for physical structures as well.

In order to check this, the simplest case of a discontinuity in both ε_r and μ_r (both of them being purely real) is considered. We again use the parallel-plate waveguide of Fig. 3, but replacing the former PML area by a material with real permittivity and permeability values of $\varepsilon_r=\mu_r=4.0$. Thus, the characteristic impedance remains unchanged, we have zero reflection theoretically, and any reflections observed can be attributed to the interface.

Tab. I presents the results of the FDFD calculation. Reflections in the range –30..-50 dB are observed, also for the non-PML substrates.

f / GHz	1	10	25
Partly substrate-filled parallel plate waveguide ($\varepsilon_r=\mu_r=4.0$) :			
S_{11} (FDFD)	0.000037	0.00374	0.02446
S_{11} (analyt.)	0.000037	0.00371	0.02316
Partly PML-filled parallel plate waveguide ($r_{th}=0.0001$):			
S_{11} (FDFD)	0.00513	0.00560	0.00764
S_{11} (analyt.)	0.00518	0.00565	0.00767

Table I Reflection coefficient of the structure in Fig. 3, with PML and with PML region replaced by lossless substrate ($\varepsilon_r=\mu_r=4.0$): FDFD results and analytical model of eqn. (3).

We conclude from this that residual reflections are not a PML-inherent effect but related to the simultaneous change of ε and μ, which also occur at the interface between PML and air (and PML sections of different conductivity). The principal reason is known. It is the staggered grid of the Yee scheme. Usually, the electric field grid is used to formulate the equations and to define the material properties, which can lead to accuracy problems when including steps in permeability, which basically is defined within the staggered magnetic cells.

As result of a systematic investigation we find empirically that the following formula describes the observed reflection errors with good accuracy:

$$S_{11} = \left| \frac{1}{4}\omega^2\mu_0\varepsilon_0\left(\frac{\Delta z}{2}\right)^2\left(\varepsilon_r^2 - 1\right)\right|, \qquad (3)$$

with ε_r to be replaced by the complex term $\varepsilon_r - j\kappa/(\omega\varepsilon_0)$ for the PML case. As can be seen from the data in Tab. I, the residual reflections caused by the interface can be estimated with excellent accuracy. Hence eqn. (3) provides a helpful tool for the practitioner in the field how to choose discretization and PML parameters in order to meet a desired maximum level of reflection errors. Further work is in progress, to develop PMLs optimized with regard to the theoretical reflection coefficient and the given reflection at the interface.

VIII. Conclusions

Our results on the PML implementation into the 3D-FDFD method can be summarized as follows: Using the anisotropic PML formulation one achieves reflection errors below -40…-50dB, which is sufficient for most practical situations.

But, this value represents a lower limit that cannot be overcome simply by varying the common PML parameters, i.e., nominal reflection factor, number of layers, and conductivity profile. The only way to reduce the reflection error is to refine discretization. This, however, is computationally expensive.

A simple test structure is used to explore PML accuracy in detail. We find that the reflections originate at the interface between PML and non-PML area, which involves a discontinuity in both complex ε and μ. This causes problems with regard to the staggered grid.

An estimation formula, valid for real and complex impedance steps, is found, to predict the magnitude of these reflections. Further work is in progress to find optimum constitutive parameters for the FDFD PML.

References

[1] J.-P. Berenger, “A Perfectly Matched Layer for the Absorption of Electromagnetic Waves,” *J. Comp. Physics* Vol. 114, pp. 185-200, 1994.

[2] Z. S. Sacks, D. K. Kingsland, R. Lee, J.-F. Lee, “A Perfectly Matched Anisotropic Absorber for Use as an Absorbing Boundary Condition,” *IEEE Trans. Antennas Propagat.*, Vol. 43, No. 12, Dec. 1995.

[3] M. Kuzuoglu and R. Mittra, “Frequency dependence of the constitutive parameters of causal perfectly matched anisotropic absorbers,” *IEEE Microwave and Guided Wave Letter*s, Vol. 6, No. 12, pp. 447–449, Dec. 1996

[4] S. D. Gedney, “An Anisotropic Perfectly Matched Layer-Absorbing Medium for the Truncation of FDTD Lattices,” *IEEE Trans. Antennas Propagat.*, Vol. 44, No. 12, pp. 1630-1639, Dec. 1996.

[5] M. R. Lyons, A. C. Polycarpou, C. A. Balanis, “On the Accuracy of Perfectly Matched Layers using a Finite Element Formulation,” *IEEE MTT-S Int. Microwave Symp. Dig.*, 1996, pp. 205–208

[6] J.-P. Berenger, “Optimized PML for wave-structure interaction problems,” PIERS, Innsbruck / Austria, July 7-12, 1996.